*34th EPS Conference on Plasma Phys. Warsaw, 2 - 6 July 2007 ECA Vol.**31F**, P-2.080 (2007)*

Aspects of self-similarity of the filamentation instability

M.E. Dieckmann[1,2], I. Lerche[1], P.K. Shukla[1] and L.O.C. Drury[2]

[1] *Faculty of Physics & Astronomy, 44780 Bochum, Germany*

[2] *Dublin Institute for Advanced Studies, Dublin, Ireland*

Abstract

The filamentation instability (FI) is an aperiodically growing instability driven by counterpropagating electron beams. Its ability to generate magnetic fields is important for the energetic plasmas in gamma ray burst jets [1] and inertial confinement fusion plasmas [2]. The FI has been examined both analytically and with particle-in-cell (PIC) simulations [3, 4, 5]. We perform [6] PIC simulations and follow the FI through its nonlinear saturation. The power spectrum of the flow-aligned current component is self-similar during the linear phase [7].

We show that the perpendicular current distribution is self-similar during the nonlinear evolution and that the filament size increases linearly with time. We demonstrate that, at least for warm plasmas, the current filaments can't be described by simple flux tubes [3, 5]. Instead, the filaments merge by magnetic reconnection to form larger, partially overlapping current sheets. In the filament overlap region the electrons are accelerated.

The physical model

FI's can be driven by electron distributions of the form $f(\mathbf{v}) = f(v_x)\,f(v_y)\,(f[v_z+v_b]+f[v_z-v_b])$, where the $f(v_j)$ are Maxwellian distributions and the beams have the mean velocity vectors $\pm\mathbf{v}_b = v_b\,\mathbf{e}_z$. We consider equally dense beams that have a temperature of 10 keV and $v_b = c/\sqrt{2}$. Such distri-

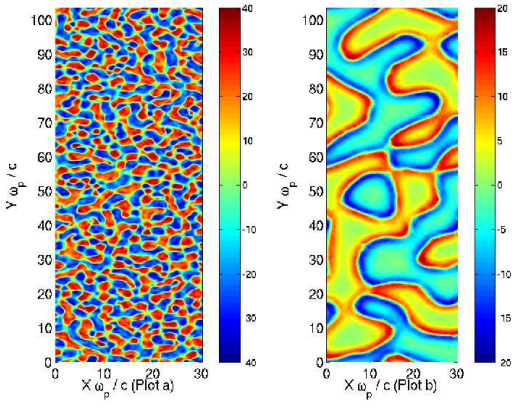

Figure 1: The distribution $C_z = \mathbf{J}\cdot\mathbf{e}_z$: The distribution just after the instability's saturation is displayed in the left panel. It is shown for T_M in the right panel.

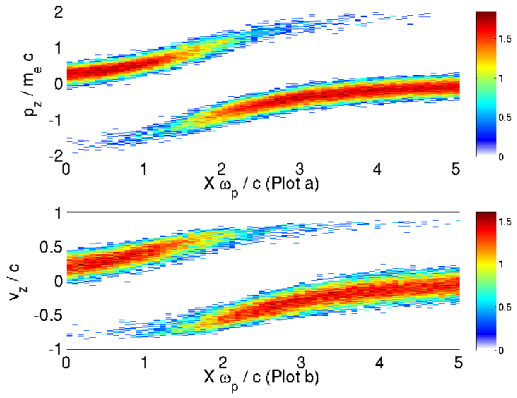

Figure 2: The electron p_z momentum (a) and v_z velocity (b) distributions at $t \approx T_M$. The electron distribution is integrated over a spatial interval with the width $0.5c/\omega_p$ along y. For the selected y a filament boundary is crossed along x.

butions favor the growth of waves with wavevectors $\mathbf{k} \perp \mathbf{v}_b$ [8]. We examine the FI with a PIC code that solves the Maxwell equations and the Lorentz equation for a large number of computational particles

$$\nabla \times \mathbf{B} = \mu_0 \mathbf{J} + \varepsilon_0 \mu_0 \frac{\partial \mathbf{E}}{\partial t}, \quad (1)$$

$$\nabla \times \mathbf{E} = -\frac{\partial \mathbf{B}}{\partial t}, \quad (2)$$

$$\frac{d\mathbf{p}_i}{dt} = q_c (\mathbf{E} + \mathbf{v}_i \times \mathbf{B}), \quad \frac{d\mathbf{x}_i}{dt} = \mathbf{v}_i. \quad (3)$$

The particles and the fields interact through the current $\mathbf{J}$. The three-dimensional field vectors are defined on a 2D grid. Since all components of $\mathbf{p}_i = m_c \Gamma_i \mathbf{v}_i$ are updated, the code is 2(1/2) dimensional. Our simulation scheme [9] fulfils $\nabla \cdot \mathbf{E} = \rho/\varepsilon_0$ and $\nabla \cdot \mathbf{B} = 0$ to round-off precision.

The grid has 1400×1400 cells and 3×10^8 computational electrons represent each of the initially spatially homogeneous beams. The runtime is $T_M = 118/\omega_p$, with $\omega_p = \sqrt{e^2 n_e / m_e \varepsilon_0}$. Initially $\mathbf{E} = 0$ and $\mathbf{B} = 0$. For more details, see Ref. [6].

The Fig. 1 shows the current component C_z in the simulation with its side length $L \times L$ with $L = 104\, c/\omega_p$. The filaments merge to non-circular sheets, which permit for a partial spatial overlap of the electron beams moving with $\pm v_b$. The electrons accelerate in these layers, as Fig. 2 demonstrates.

A Fourier transformation over x and y is applied to the spatial distributions of the currents C_z and $C_x + iC_y$ for a sequence of equal time intervals. The power spectra are $|FT(C_z)|^2$ and $|FT(C_x + iC_y)|^2$ and they are integrated in the k_x, k_y plane over the azimuth angle [6]. The k-spectrum of C_z is displayed in Fig. 3 and that of $C_x + iC_y$ in Fig. 4.

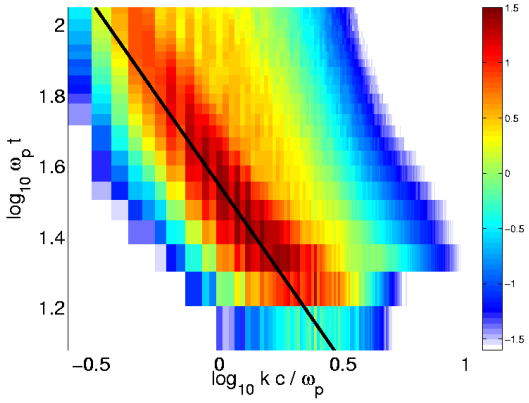

Figure 3: The 10-logarithmic k-spectrum of C_z. Overplotted is a line $k \sim t^{-1}$, which follows the maximum of the power.

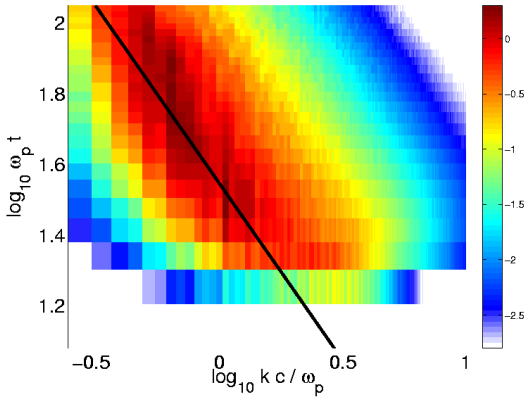

Figure 4: The 10-logarithmic k-spectrum of $C_x + iC_y$. Overplotted is a line $k \sim t^{-1}$, which follows the maximum of the power.

Both spectra demonstrate that the scale size of the current filaments increases linearly with t. The spectrum of C_z is a power-law, when the FI saturates [6, 7]. A power-law distribution with a constant slope gives parallel contour lines. During the filament merging, such lines can't be seen in Fig. 3.

Instead, the $C_x + iC_y$ component in Fig. 4 shows parallel contour lines at large k. The power-law presumably arises from preferential attachment of filaments, since the probability for attachment increases with the filament perimeter [6]. Since the filaments repel each other through magnetic fields, the filament merger must be accompanied by magnetic field line reconnection. The current annihilation due to the beam overlap in Fig. 2 is known to trigger reconnection [10]. Indeed, the Fig. 5 shows one of many magnetic x-points in the simulation plane.

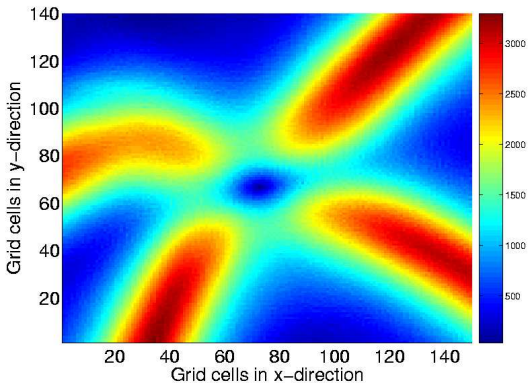

Figure 5: A magnetic x-point in the simulation at $t \approx T_M$: The color scale shows $\sqrt{B_x^2 + B_y^2}$. The spatial units are grid cells, demonstrating the high resolution that is necessary to accurately represent the reconnection process.

Summary

- The FI results in the formation of non-circular current filaments, that repel or attract each other. The ones that attract each other merge and increase their size linearly with t.
- The power spectrum of the current distribution in the simulation plane shows a power-law at high-k, presumably due to preferential filament attachment.
- When the filaments merge, the magnetic field lines confining them must reconnect. This reconnection requires a high simulation resolution.

Acknowledgements

This work has been financially supported by the Deutsche Forschungsgemeinschaft (DFG) and the Dublin Institute for Advanced Studies (DIAS). The Swedish High-Performance Computer Centre North has provided the computer facilities and support.

References

[1] M.V. Medvedev and A. Loeb, Astrophys. J. **526**, 697 (1999)

[2] M. Tabak et al., Phys. Plasmas **12**, 057305 (2005)

[3] T.J. Bogdan and I. Lerche, Astrophys. J. **296**, 719 (1985)

[4] M. Honda, J. Meyer-ter-Vehn and A. Pukhov, Phys. Plasmas **7**, 1302 (2000)

[5] M.V. Medvedev et al., Astrophys. J. **618**, L75 (2005)

[6] M.E. Dieckmann, I. Lerche, P.K. Shukla and L.O.C. Drury, New J. Phys. **9**, 10 (2007)

[7] J.T. Frederiksen, C.B. Hededal, T. Haugbolle and A. Nordlund, Astrophys. J. **608**, L13 (2004)

[8] A. Bret, M.E. Dieckmann and C. Deutsch, Phys. Plasmas **13** 082109 (2006)

[9] J.W. Eastwood, Comput. Phys. Comm. **64** 252 (1991)

[10] G.L. Eyink and H Aluie, Physica D **223** 82 (2006)